Dynamics of Sodium Ions and Water in Swollen Superabsorbent Hydrogels as Studied by ^{23}Na- and ^{1}H-NMR

Xiaoai Guo, Solveig Theissen, Jan Claussen, Viet Hildebrand, Juliane Kamphus, Manfred Wilhelm, Burkhard Luy, and Gisela Guthausen**

Dynamics of sodium ions and water in swollen superabsorbent polymer (SAP) hydrogels are studied by ^{23}Na- and ^{1}H-NMR, respectively. The apparent diffusion coefficients of water in swollen SAPs, probed by ^{1}H pulsed field gradient NMR, decreases with increasing diffusion time. The degree of hindrance depends on structural and synthesis parameters. It is quantified within a tortuosity model. Based on the results, the swelling degree has the highest impact on the ion mobility, apart from synthesis parameters leading to different levels of physical and chemical crosslinks. ^{23}Na-NMR relaxation and diffusion reveal the $^{23}Na^{+}$ mobility in swollen SAPs. A higher degree of neutralization leads to faster relaxation and to a smaller apparent diffusion coefficient. Surface crosslinking restricts water mobility, but has a smaller impact on the dynamics of sodium ions. The experimental results indicate an influence of SAP structure on the dynamics of ions and water molecules.

1. Introduction

Hydrogels, such as superabsorbent polymers (SAPs), attracted considerable scientific and industrial interest because their hydrophilic networks can absorb and retain large amounts of water.[1–3] The swelling capacity of SAPs depends on the degree of crosslinking, that is, synthesis parameters, and ion concentration in the aqueous solutions. For instance, SAP hydrogels can be designed as "core-shell" particles with a lower core crosslink density covered by a surface layer with a higher crosslink density to achieve high liquid absorbance and retention capacity while avoiding gel blocking.[4] In general, the superabsorbance results from the combination of hydration, swelling, and diffusion.[5] Hydrogen bonds and electrostatic interactions play a major role.[6] The crosslinking density of a SAP network directly influences the level of swelling and the strength of the network. In addition, the polymer chains contain negatively charged carboxylate groups, which are neutralized by monovalent positive counterions. The hydration shell of $^{23}Na^{+}$ weakens the interaction between the ions and the carboxylate groups. The difference in the osmotic pressure inside and outside the SAP matrix will also influence water diffusion in a swollen gel. Thus, the final diffusion within polymer networks depends on concentration and swelling degree.[7,8]

Translational motion of $^{23}Na^{+}$ and water in swollen SAP hydrogels is influenced by the often inhomogeneous polymer network, which is closely related to the synthesis parameters such as degree of neutralization, monomer concentration, degree of crosslinking, and surface crosslinking as well as particle size and shape.[9,10] Thus water and ions, that is, diffusing moieties, may be distributed throughout the swollen polymer networks in a nonuniform way. To study and understand the translational motion of the diffusing moieties within the network is scientifically interesting because the translational motion not only reflects intrinsic properties of molecules themselves but also elucidates their environment, for example, intermolecular dynamics or motional restriction.[11] Translational dynamics, that is, diffusion, of guest moieties in swollen SAPs primarily depends on the confinement by the polymer network and the electrostatic interactions.

Pulsed field gradient NMR (PFG-NMR) is known to be a powerful noninvasive technique to study translational diffusion in polymer gels.[12,13] PFG-NMR measures the apparent diffusion coefficient as a function of diffusion time. Although there are numerous studies on diffusion in various porous materials,[14–17] to the best of our knowledge there are few reports on the time-dependent hindered diffusion in swollen SAPs.[18]

Dr. X. Guo, Prof. M. Wilhelm
Institute for Chemical Technology and Polymer Chemistry
Karlsruhe Institute of Technology
Engesserstrasse 18, 76131 Karlsruhe, Germany
E-mail: xiaoai.guo@kit.edu
S. Theissen, Prof. G. Guthausen
Institute for Mechanical Process Engineering and Mechanics
Engler-Bunte-Institut, Chair of Water Chemistry and Water Technology
Karlsruhe Institute of Technology
Adenauerring 20b, 76131 Karlsruhe, Germany
E-mail: gisela.guthausen@kit.edu
Prof. B. Luy
Institute of Organic Chemistry and Institute for Biological Interfaces 4
Karlsruhe Institute of Technology
Fritz-Haber-Weg 6, 76131 Karlsruhe, Germany
Dr. J. Claussen, Dr. V. Hildebrand, Dr. J. Kamphus
Procter & Gamble Service GmbH
Sulzbacher Strasse 40, 65824 Schwalbach am Taunus, Germany

The purpose of this work is to study the dynamics of $^{23}Na^{+}$ and water in swollen SAPs, which helps us to better understand the impact of hydrogel topology on the dynamics of ions and molecules in the swollen gels. This is of essential importance for further development and application of new SAP materials. ^{1}H- and ^{23}Na-PFG-NMR diffusion and ^{23}Na-relaxation experiments on SAPs with different synthesis parameters have been performed at different swelling degrees. Hindrance by the SAP networks on the translational mobility and the correlation of NMR results with structural and synthesis parameters are discussed.

2. Experimental Section

2.1. Materials and Sample Preparation

SAP hydrogels based on acrylic acid were synthesized by Procter & Gamble Service GmbH (Schwalbach, Germany)[9] (**Table 1**) and were investigated by ^{1}H- and ^{23}Na-PFG-NMR diffusion and ^{23}Na-relaxation. The SAP samples were named on the basis of synthesis parameters (Table 1) as "SAP DN|AA|DC" and "SAP DN|AA|DC|RSXL," where AA, DN, DC denote monomer concentration, degree of neutralization, and degree of crosslinking, respectively. R refers to the synthesis with a different reactor type and RSXL to the sample with surface crosslinking, respectively. NMR samples were prepared by filling the dry powder in a 5 mm NMR glass tube and subsequently mixing with Milli-Q water at defined mass ratios ($m_{SAP} : m_{H_2O}$ = 1:5, 1:9, 1:15, and 1:20). To avoid water evaporation, the filled tubes were sealed with parafilm. The samples were left to swell and equilibrate for more than 24 h before performing NMR measurements. The filling level of the NMR glass tube was between 8 and 10 mm to locate the sample in the center of the radio frequency coil within the relatively homogeneous B_1 field in the minispec. In addition, a dilute (0.1 M) and a supersaturated aqueous solution of NaCl were prepared for comparison. In the latter, some undissolved NaCl crystals were visible at the bottom of the NMR tube.

Table 1. Properties of the acrylic acid–based SAP hydrogels. Adapted with permission.[9] Copyright 2018, Wiley-VCH.

Hydrogel samples SAP DN|AA|DC	DN [mol%]	AA [wt%]	DC [mol%]	Symbols[c)]
SAP 75|20|0.3	75	20	0.3	□
SAP 75|25|0.3	75	25	0.3	∇
SAP 75|30|0.3	75	30	0.3	◊
SAP 75|20|1	75	20	1.0	○
SAP 75|25|1	75	25	1.0	Δ
SAP 100|25|0.3	100	25	0.3	◁
SAP 100|25|1	100	25	1.0	▷
SAP 75|20|0.3|R[a)]	75	20	0.3	⊕
SAP 75|20|0.3|RSXL[b)]	75	20	0.3	⊟

[a)]Synthesis with a different reactor type compared to SAP 75|20|0.3. The sample was used as a reference for SXL SAP; [b)]Synthesis with a different reactor type, surface crosslinked SAP (RSXL); [c)]Symbols used in the figures; DN, degree of neutralization, defined as the mole ratio of NaOH to acrylic acid; AA, solid content, that is, monomer concentration at the beginning of polymerization, defined as the mass ratio of polymer synthesis educts to water; DC, degree of crosslinking, defined as the mole ratio of crosslinker methylenebisacrylamide to acrylic acid.

2.2. NMR Methods and Instrument

The ^{23}Na and ^{1}H PFG-NMR diffusion experiments were performed at 25 °C on a 400 MHz NMR spectrometer (Bruker Avance 400 WB, Bruker, Germany) at 9.4 T (^{23}Na Larmor frequency 106 MHz). It was equipped with a diffusion probe DIFF BB, providing a maximum gradient amplitude g up to 12 T m^{-1} when using a 40 A gradient amplifier. The spectra were measured via PFG-STE with 32 linearly incremented gradients and 6–16 scans.[12] The measured signal decay was interpreted in terms of S/S_0 versus q^2, where S_0 is the signal intensity at $q = 0$. q is defined as the product $\gamma g\delta/2\pi$, where γ is the magnetogyric ratio, and δ is the gradient pulse duration (**Table 2**). As the data show not only the self-diffusion of the moieties, the data processing step had to be considered, that is, the monoexponential Stejkal and Tanner description (Equation (1)) and a gamma distribution model (Equations (2) and (3)) were used to describe the signal decays.[19–21]

$$\frac{s(q)}{s_0} = \exp[-Dq^2(\Delta - \delta/3)] \tag{1}$$

Δ is the diffusion time and D the diffusion coefficient. In complex mixtures and geometric hindrance, the signal decay can be described using a gamma distribution $P_G(D)$ function.

$$\frac{s(q)}{s_0} = \int_0^\infty P_G(D)\exp[-Dq^2(\Delta - \delta/3)]\, dD \tag{2}$$

$$P_G(D) = \frac{D^{\kappa-1}\exp(-D/\theta)}{\Gamma(\kappa)\theta^{\kappa}} \tag{3}$$

The mean value $D_{mean} = \theta\kappa$ and the width of the distribution $\sigma = \theta\sqrt{\kappa}$ describe the distribution function, while θ is

Table 2. Parameters of ^{23}Na and ^{1}H PFG-NMR.

Method	Parameter	Value
^{23}Na PFG-NMR	Gradient pulse duration, δ	2 ms
	Maximum gradient value used, g_{max}	9 T m^{-1}
	Number of gradient steps	32
	Diffusion time for swollen hydrogels, Δ	7–30 ms
	Diffusion time for 0.1 M NaCl solution, Δ	7–50 ms
	Repetition time	2 s
^{1}H PFG-NMR	Gradient pulse duration, δ	3 ms
	Maximum gradient value used, g_{max}	0.6 T m^{-1}
	Number of gradient steps	32
	Diffusion time, Δ	40–480 ms
	Repetition time	2.5 s

a scaling parameter. κ is a shape factor, and Γ is the gamma function.

Longitudinal ^{23}Na-NMR relaxation rates ($R_1 = 1/T_1$) were measured using the inversion-recovery sequence with 16 recovery delays. Transverse relaxation ($R_2 = 1/T_2$) was measured by the Carr–Purcell–Meiboon–Gill (CPMG) sequence with 32 echoes and an echo time of 200 μs.[22,23] The phase corrected data acquired within Topspin 2.1 (Bruker, Germany) were integrated in the significant regions of the spectra. Further data processing was done using home-written Matlab routines.

3. Results and Discussion

3.1. Diffusion of $^{23}Na^+$ Ions in Swollen SAP Hydrogels

PFG-STE-NMR has been applied to study translational dynamics of $^{23}Na^+$ (spin-3/2) and water in the swollen SAP hydrogels. The nuclear electric quadrupole moment (Q = 10.4 fm^2) of ^{23}Na is relatively large. ^{23}Na-NMR spectra of solids often show quadrupolar splittings and broadening, while in liquids the random motion of $^{23}Na^+$ usually averages out the static electric field gradient, leading to narrow lines.

Figure 1a exemplarily shows ^{23}Na 1 D NMR spectra for a swollen hydrogel (SAP75|20|0.3|R) and a supersaturated NaCl solution. Besides a sharp peak from mobile $^{23}Na^+$, an asymmetric and broad line is observed for the supersaturated NaCl solution. This is due to the residual quadrupolar interaction in undissolved NaCl in the supersaturated solution. The broad peak is not observed in the ^{23}Na NMR spectrum of the swollen hydrogel (Figure 1a), nor in the other swollen SAPs. A time average is observed in the ^{23}Na NMR spectrum, and no static quadrupolar broadening occurs, indicating fast ion dynamics.

The peak intensity S in the ^{23}Na PFG-STE-NMR spectrum of a swollen hydrogel (SAP75|20|0.3|R) (Figure 1b) decreases with increasing gradient amplitude g. The signal decays S/S_0 versus q^2 for the swollen hydrogel with surface crosslinking (SAP75|20|0.3|RSXL) and a dilute NaCl solution (0.1 M) indicate different diffusion coefficients (Figure 1c). Both the monoexponential decay and the gamma distribution model describe the ^{23}Na diffusion data well for all investigated SAP hydrogels within the experimental accuracy. A difference in the signal decays for the SAP hydrogels with and without surface crosslinking was observed. $^{23}Na^+$ ions in swollen hydrogels have similar diffusion properties except for a small influence of surface crosslinking. In contrast, the signal decay for 0.1 M NaCl solution has a steeper slope, that is, $^{23}Na^+$ diffuses much faster in the dilute solution than in the swollen hydrogels.

$^{23}Na^+$ effective diffusion coefficients were measured in a rather limited range of diffusion times Δ, restricted by the $^{23}Na^+$ longitudinal relaxation time, for example, T_1 = 49.6 ms for the dilute NaCl solution. The diffusion coefficients D_{Na^+} in the SAP hydrogels at a swelling mass ratio of 1:5 are about half of the value ($D_{0,Na^+} = 1.05\times10^{-9}$ s^{-1}) of freely diffusing $^{23}Na^+$ in

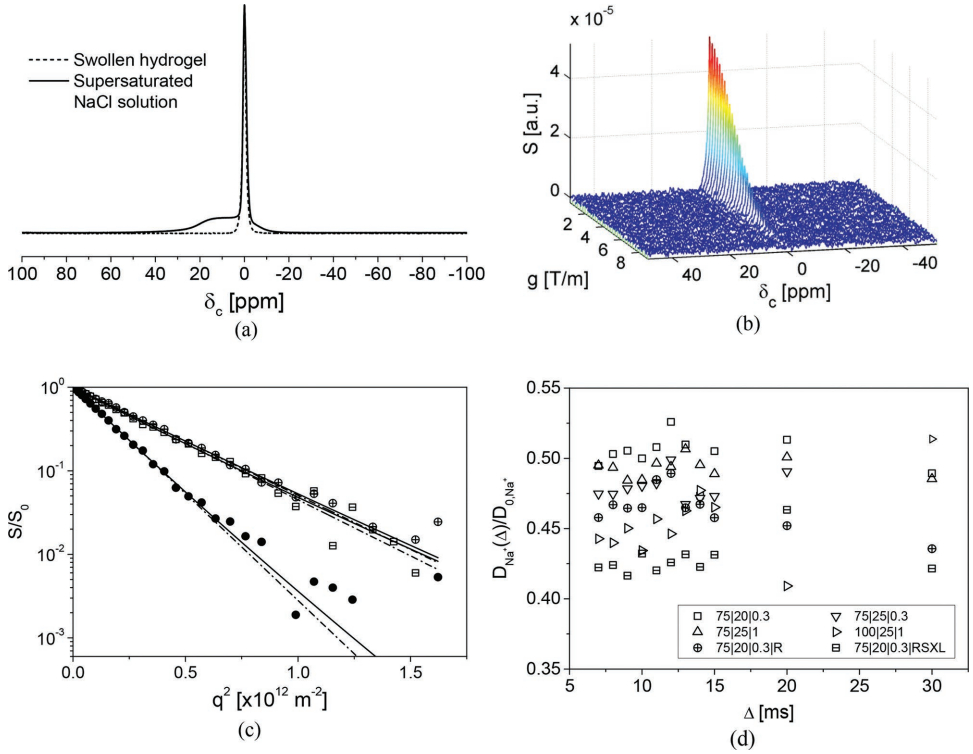

Figure 1. a) ^{23}Na 1D NMR spectra for a swollen hydrogel (SAP75|20|0.3|R) and a supersaturated NaCl solution; b) ^{23}Na PFG-STE-NMR spectrum for a swollen hydrogel (SAP75|20|0.3|R); c) mono-exponential (dot-dashed lines) and gamma distribution model (solid lines) describe the signal decays S/S_0 for the diffusion of ^{23}Na ions in the swollen hydrogels (⊕, 75|20|0.3|R; ⊟, 75|20|0.3|RSXL) and a 0.1 M NaCl reference solution (●) within the experimental accuracy; d) $^{23}Na^+$ diffusion coefficients D_{Na^+} in SAPs (1:5), normalized to D_{0,Na^+} of $^{23}Na^+$ in the 0.1 M NaCl reference solution as a function of diffusion time Δ.

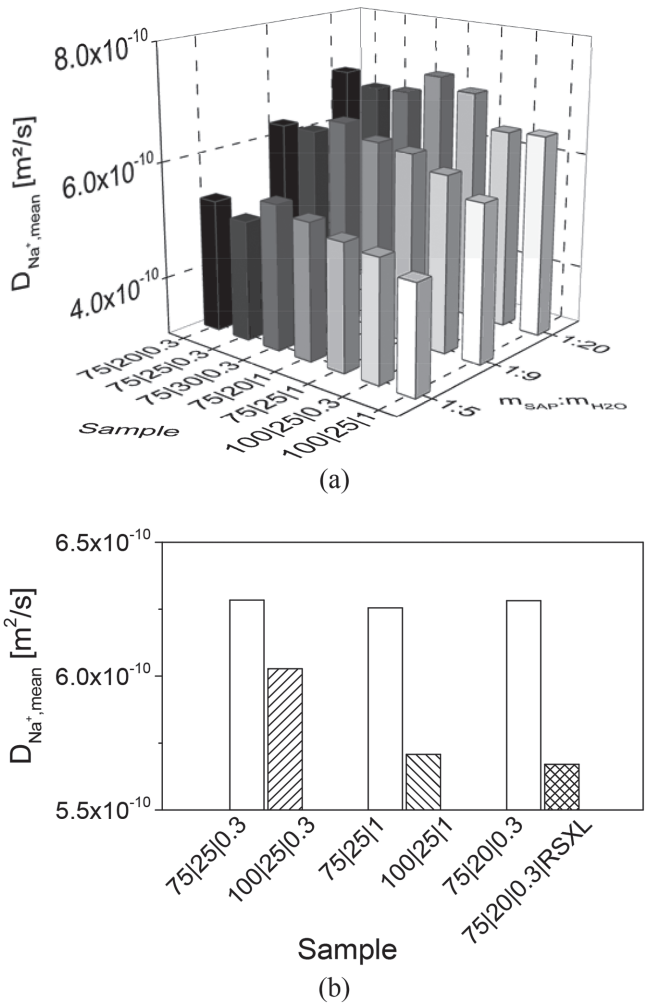

Figure 2. a) $^{23}Na^+$ mean diffusion coefficients for SAP hydrogels at three different swelling degrees ($m_{SAP}:m_{H_2O}$ = 1:5, 1:9, and 1:20); b) $^{23}Na^+$ mean diffusion coefficients for different DN as well as for surface crosslinking RSXL.

the 0.1 M NaCl solution (Figure 1d). This value is in good agreement with the value of 1.04 × 10^{-9} m^2 s^{-1} in literature.[24,25] Hydrogels with a high DN and surface crosslinking show smaller diffusion coefficients, suggesting a hindering influence of surface crosslinking on the $^{23}Na^+$ diffusion. D_{Na^+} remained nearly constant for $\Delta \in [7, 30]$ ms (i.e., the diffusion time Δ in the range 7–30 ms) within the experimental error. Similar characteristics were observed by PFG-NMR in a previous study on resins swollen with water,[26] where $^{23}Na^+$ diffusion coefficients were found to be constant for $\Delta \in [3,25]$ ms.

With increasing swelling degree Q, $^{23}Na^+$ ions diffuse faster (**Figure 2**a). In addition, the effective $^{23}Na^+$ diffusion coefficients for samples with higher DN and the same AA and DC are somewhat smaller (cf. SAP**100**|25|0.3 versus SAP**75**|25|0.3, and SAP**100**|25|1 versus SAP**75**|25|1 in Figure 2b). An increase in $^{23}Na^+$ concentration, that is, DN, tends to increase the degree of adsorption of $^{23}Na^+$ on -COO^- of the polymer chains.[27–30] Comparing the "core-shell" hydrogel with surface crosslinking to that without surface crosslinking (cf. SAP75|20|0.3|RSXL versus SAP75|20|0.3 in Figure 2b) reflects the swelling constraints caused by the surface crosslinking. Both parameters, that is, DN and surface crosslinking lead to smaller diffusion coefficients. However, there is almost no difference in $D_{Na^+,mean}$ for hydrogels with different AA and DC (cf. SAP75|**25**|**0.3**, SAP75|**25**|**1**, and SAP75|**20**|**0.3** in Figure 2b). A similar trend has been observed at other swelling degrees (Figure 2a), which have a higher impact on self-diffusion than the synthetic parameters AA, DC, and DN.

3.2. Diffusion of Water in Swollen SAP Hydrogels: Modeling and Comparison of SAPs

Compared to the $^{23}Na^+$ PFG-signal decays (Figure 1c) and pure water (**Figure 3**a), the hydrogel sample with surface crosslinking exhibits the slowest signal decay in ^1H PFG-NMR. The signal decay curve concaves upward and deviates from the mono-exponential function at larger q^2 (cf. ⊟, dotted curve in Figure 3a). This indicates a strong hindrance of the water mobility in swollen hydrogels, resulting in a ^1H diffusion coefficient distribution. The gamma distribution model, resulting in a mean ^1H diffusion coefficient $D_{H,mean}$ and a distribution width σ, describes the signal decay with high experimental accuracy down to about the noise level in the range of $S/S_0 = 10^{-3}$–10^{-2} (Figure 3a). $D_{H,mean}$ is a function of the diffusion time Δ and was normalized to the diffusion coefficient ($D_0 = 2.299 \times 10^{-9}$ m^2/s) of pure water at 25 °C (Figure 3b).[31] $D_{H,mean}(\Delta)/D_0$ decreases with diffusion time, while $\Delta \in [30,480]$ ms. $D_{H,mean}$ approaches constant values at large Δ, which are much smaller than D_0. The samples with the same AA and DC but different DN exhibit very similar hindered diffusion (cf. SAP75|25|0.3 vs SAP100|25|0.3), whereas samples with higher DC show smaller water diffusion coefficients, that is, stronger hindering effects of network structures (cf. SAP75|20|**1** vs SAP75|20|**0.3** and SAP75|25|**1** vs SAP75|25|**0.3**). Similar effects of DC on the diffusion of water molecules in SAP hydrogels have also been observed in previous studies on polymer gels such as poly(methacrylic acid).[32,33] Among the SAPs under study, the sample with surface crosslinking has the smallest water diffusion coefficient due to swelling restriction in the "core-shell" particles.

Solid lines in Figure 3b represent fits of a tortuosity model (Equation (4)[34]), to estimate the tortuosity $\mathcal{T}$ in swollen hydrogels.

$$\frac{D(\Delta)}{D_0} = 1 - \left(1 - \frac{1}{\mathcal{T}}\right) \cdot \frac{a\sqrt{\Delta} + b(1 - 1/\mathcal{T}) \cdot \Delta}{(1 - 1/\mathcal{T}) + a\sqrt{\Delta} + b(1 - 1/\mathcal{T}) \cdot \Delta} \quad (4)$$

where a and b are fitting parameters which depend on the hydrogel. The asymptotic value $\lim_{\Delta \to \infty} D(\Delta)/D_0$ is related to the inverse of tortuosity,[11] which describes the average geometrical hindrance in the swollen hydrogel relative to the obstacle- and interaction-free pure water. The tortuosity approaches $\mathcal{T} = 1$ in the limit of pure water without geometric hindrance of polymers or molecular interactions.[35,36]

$D_{H,mean}(\Delta)/D_0$ for hydrogels without and with surface crosslinking was described in this model at different swelling degrees, respectively (Figure 3c,d). Solid lines represent fits of Equation (4) to the data to estimate the tortuosity in the

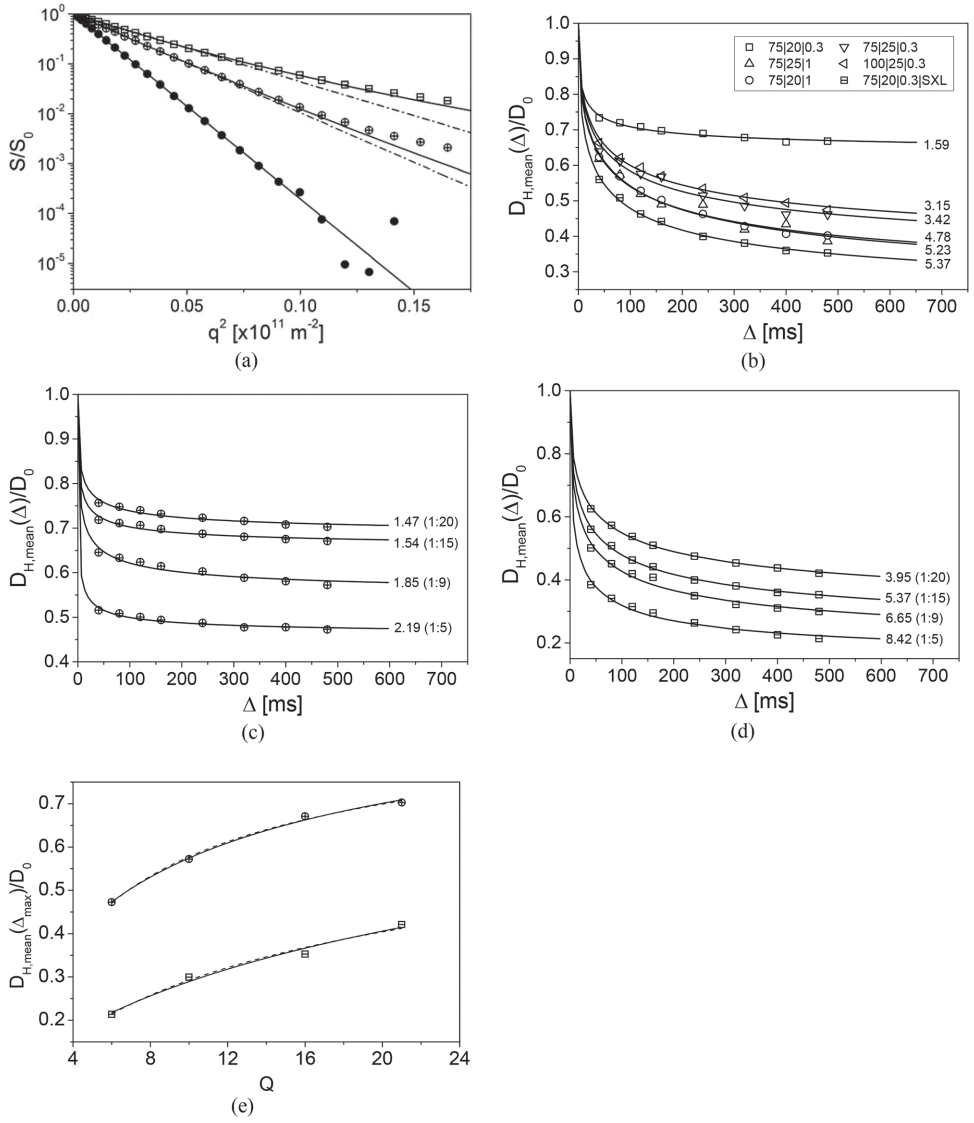

Figure 3. a) ^{1}H PFG-NMR signal decays S/S_0 in the (non-)surface-crosslinked hydrogels (⊕, 75|20|0.3|R; ⊟, 75|20|0.3|RSXL) and pure water (●) were modeled by the mono-exponential function (dot-dashed lines) and the gamma distribution model (solid lines); b) $D_{H,mean}(\Delta)/D_0$ depends on diffusion time Δ. Tortuosities [fits of Equation (4), solid lines and numbers in the graphs] are given in addition. c) $D_{H,mean}(\Delta)/D_0$ in a non-surface-crosslinked hydrogel (SAP75|20|0.3|R) at different swelling degrees; d) $D_{H,mean}(\Delta)/D_0$ in a surface-crosslinked hydrogel (SAP75|20|0.3|RSXL) at different swelling degrees; e) $D_{H,mean}(Q,\Delta_{max})/D_0$ modeled as a function of Q based on Phillies model (dashed lines) and Petit model (solid lines).

swollen hydrogels. The model describes the time-dependent diffusion data very well which is also reflected in the error analysis (**Table 3**). Obviously surface crosslinking leads to a faster reduction of $D_{H,mean}(\Delta)$ because of stronger hindrance. With increasing swelling degree, the hydrogel networks expand more, and hindrance decreases. The volumetric expansion allows water molecules to diffuse faster inside the gel, leading to larger diffusion coefficients (cf. Figure 3c,d).

In swollen SAPs, water molecules are hindered in their diffusion by the obstructing network. Because of the geometrical restriction, the measured ^{1}H diffusion coefficient decreases with diffusion time Δ (Figure 3) and gradually approaches a plateau value, which can be related to the tortuosity $\mathcal{T}$.[11] Time-dependent diffusion coefficients of fluids in porous media have often been used to measure the pore size distribution and surface-to-volume ratio of pores.[16,34,37] Crosslinked networks are different from conventional porous materials, for example, porous stones and porous coordination polymers[38,39] as "pores" are difficult to be defined. A probably more appropriate way to model the time dependence of the mean diffusion coefficient is to consider the interactions of a guest moiety with polymers and the geometric hindrance by the polymers. Various theoretical and physical models for diffusion of solvents and/or solutes in polymer systems under different circumstances, modifications, and improvements on the existing theories as well as the use of models in the interpretation of diffusion have been published.[7,40] Previous experiments on fluid-saturated packed beds and on a biological sample showed

Table 3. Error analysis for the fit of tortuosity model [Equation (4)] to the ^{1}H diffusion data in the (non-)surface-crosslinked hydrogels.

Sample	Swelling ratio	Fit of tortuosity model			Fit error	
		Parameter a	Parameter b	Tortuosity $\mathcal{T}$	Standard error	Maximum deviation
75|20|0.3|R	1:5	6.24E-01	1.16E-05	2.19	5.56E-03	5.95E-03
	1:9	2.17E-01	6.21E-06	1.85	1.02E-02	1.10E-02
	1:15	1.98E-01	1.67E-05	1.54	7.06E-03	7.95E-03
	1:20	1.40E-01	4.81E-06	1.47	6.79E-03	7.69E-03
75|20|0.3|RSXL	1:5	3.00E-01	4.18E-06	8.42	1.17E-02	1.36E-02
	1:9	1.76E-01	2.61E-06	6.65	1.61E-02	2.33E-02
	1:15	1.45E-01	2.00E-06	5.37	7.19E-03	8.63E-03
	1:20	1.14E-01	1.59E-06	3.95	5.46E-03	7.62E-03

that Equation (4) describes $D(\Delta)/D_0$ well for diffusion times up to ≈1 s. The tortuosity agreed well with the values obtained by numerical simulations.[34] Thus, the average hindrance in the SAP hydrogel relative to the obstacle-free diffusion could be modeled within the tortuosity model. Physically, the diffusing moieties move around the polymer chains which obstruct their direct mean free path. Such hindrance will make the effective distance traveled by water molecules in the swollen SAP hydrogel smaller than that traveled in the case of random Brownian motion. The data obtained for SAPs can be well described by Equation (4) (Figure 3b). SAP75|20|0.3 shows the lowest tortuosity. This is expected because smaller AA and DC result in a weaker hindrance on diffusion in the swollen gel. SAP75|25|1 shows a higher tortuosity because larger AA and DC cause a stronger hindrance. A similar diffusion pattern has been observed in SAP75|20|1 due to its larger DC. The hydrogel with surface crosslinking SAP75|20|0.3|RSXL exhibits the highest tortuosity (Figure 3b). These results are in accordance with the interpretation that the time dependence is dominated by geometric restrictions within the gel. An increase of swelling degree leads to reduced hindrance and thus to a lower tortuosity (Figure 3c,d).

To further explore the dependence of hindered diffusion on Q in swollen SAPs, $D_{\mathrm{H,mean}}(Q,\Delta_{\max})/D_0$ was modeled as a function of Q. Guest molecule diffusion in polymer systems can be described by different models, for example, the multiparameter model of Vrentas–Duda, the hydrodynamic model of Phillies, and the Petit model,[7,41–44] given by Equations (5–7), respectively.

$$\frac{D_{H,\mathrm{mean}}(Q,\Delta_{\max})}{D_0}=\exp\left\{\frac{-B_d'(1-f_p')}{(Q-1)+f_p'}\right\} \tag{5}$$

where B_d' and $f_p'=f_p/f_s$ are two dimensionless parameters. f_p and f_s are the free volumes of the polymer and solvent, respectively.

$$\frac{D_{H,\mathrm{mean}}(Q,\Delta_{\max})}{D_0}=\exp\{-\alpha Q^{-\nu}\} \tag{6}$$

where α and ν depend on the properties of the diffusing moiety and the specific polymer system, and can be considered as phenomenological parameters.[44]

$$\frac{D_{H,\mathrm{mean}}(Q,\Delta_{\max})}{D_0}=\frac{1}{1+aQ^{-2\nu'}} \tag{7}$$

where the characteristic parameters a and ν' are related to the local viscosity in the swollen SAP.

For the sake of simplicity, both the Phillies model and the Petit model have been applied to the data (Figure 3e). Both models describe the experimental data well. Hindrance decreases or the inverse of tortuosity increases with Q. Similar behavior has been observed for other swollen SAPs (**Table 4**). It is interesting to note that both fit parameters ν in Phillies model and ν' in Petit model have smaller values for the swollen SAPs with higher DC (cf. SAP75|20|**0.3** vs SAP75|20|**1**, SAP75|25|**0.3** vs SAP75|25|**1**, and SAP100|25|**0.3** vs SAP100|25|**1**), and so do the SAP with surface crosslinking. Except for SAP75|30|0.3, an increase of AA leads to an increase of ν and ν' (cf. SAP75|**20**|0.3 vs SAP75|**25**|0.3 and SAP75|**20**|1 vs SAP75|**25**|1). As pointed out by other researchers,[7,44] the physical significance of the fit parameters in various systems remains vague. Nevertheless, the present work shows that both models provide a good description of the data for different swollen SAPs within the studied range of Q. $D_{\mathrm{H,mean}}/D_0$ is related to DC and surface crosslinking. This hints at the possible swelling heterogeneity and/or change of local viscosity due to different interactions (see Section 3.3) in swollen SAPs. Both effects will impact the mobility of water in SAPs at different Q.

3.3. Interactions between Water Molecules, Counterions, and Hydrogel Network

^{1}H double-quantum NMR[9,10] indicates that guest moieties may be distributed in a nonuniform way. Water molecules

Table 4. Fit parameters of Phillies model and Petit model for various swollen SAPs.

Hydrogel samples SAP DN|AA|DC	Phillies model, Equation (6)		Petit model, Equation (7)	
	α	ν	a	ν'
SAP 75|20|0.3	1.441	0.461	2.410	0.285
SAP 75|25|0.3	3.497	0.890	8.152	0.575
SAP 75|30|0.3	1.726	0.191	4.229	0.158
SAP 75|20|1	1.461	0.213	2.824	0.162
SAP 75|25|1	2.469	0.330	7.864	0.277
SAP 100|25|0.3	3.140	0.521	10.282	0.403
SAP 100|25|1	2.677	0.350	9.490	0.305
SAP 75|20|0.3|R	2.274	0.617	4.642	0.398
SAP 75|20|0.3|RSXL	3.384	0.440	13.755	0.374

in agarose and alginate gels[45] also experience hindered diffusion. Translational motion of water in polymer gels can be quantified by diffusion. From the microscopic point of view, SAPs consist of polymer chains, crosslinkers, and extractables (e.g., residual monomers, oligomers, and non-crosslinked small polymer chains) as well as network defects such as dangling chains and loops.[46] Water molecules approach or contact polymer chains and segments, and the interactions to be named in this context are water–water bonding, water–polymer bonding, electrostatic interactions as well as water–$^{23}Na^+$ interactions. The interactions may vary, that is, water diffusion is affected in various ways and to different degrees. In PFG-NMR, an effective diffusion coefficient distribution reflects the sum of all contributions, including water molecules fast diffusing in the region far from hydrogel networks, free water at the surface, water molecules interacting with the hydrogel network or exchanging ^1H in regions close to COO^-, and water molecules crossing different regions during the observation time. For instance, the hindrance and water–polymer interaction in a region close to the polymer chain will be stronger than those in a region where water molecules experience no interaction. In other words, at a certain DC, water diffusion decreases as water molecules approach the polymer–water interface.

As already discussed, the ^1H PFG-NMR signal decays in the swollen hydrogel indicate distributions of diffusion coefficients (**Figure 4**a). To adequately describe ^1H PFG-STE-NMR data, the gamma distribution model was used. The relative distribution width $\sigma/D_{H,mean,\Delta max}$ is a measure to quantify the hindering effects of polymer network on water molecules in swollen hydrogels, and was compared with structural and synthesis parameters of SAPs (Figure 4b). ^1H-^1H residual dipolar couplings (RDC) D_{res} measured by ^1H DQ-NMR depend on polymer specific parameters like geometry, distance, and chain dynamics. D_{res} is related to synthesis parameters.[9] An increase in D_{res} is in parallel with an increase in $\sigma/D_{H,mean}(Q,\Delta_{max})$ (Figure 4b). Both parameters are related to the hydrogel network, where the surface-crosslinked SAP hydrogel exhibits a larger value of $\sigma/D_{H,mean}(Q,\Delta_{max})$ due to the higher hindrance of surface crosslinking to water mobility.

To further explore the interactions in the swollen hydrogel containing hydrophilic groups ($–COO^-$ H^+ and/or $–COO^-$ Na^+), water mobility was modeled (Figure 4c,d). The SAP hydrogel under study is an anionic polyelectrolyte with

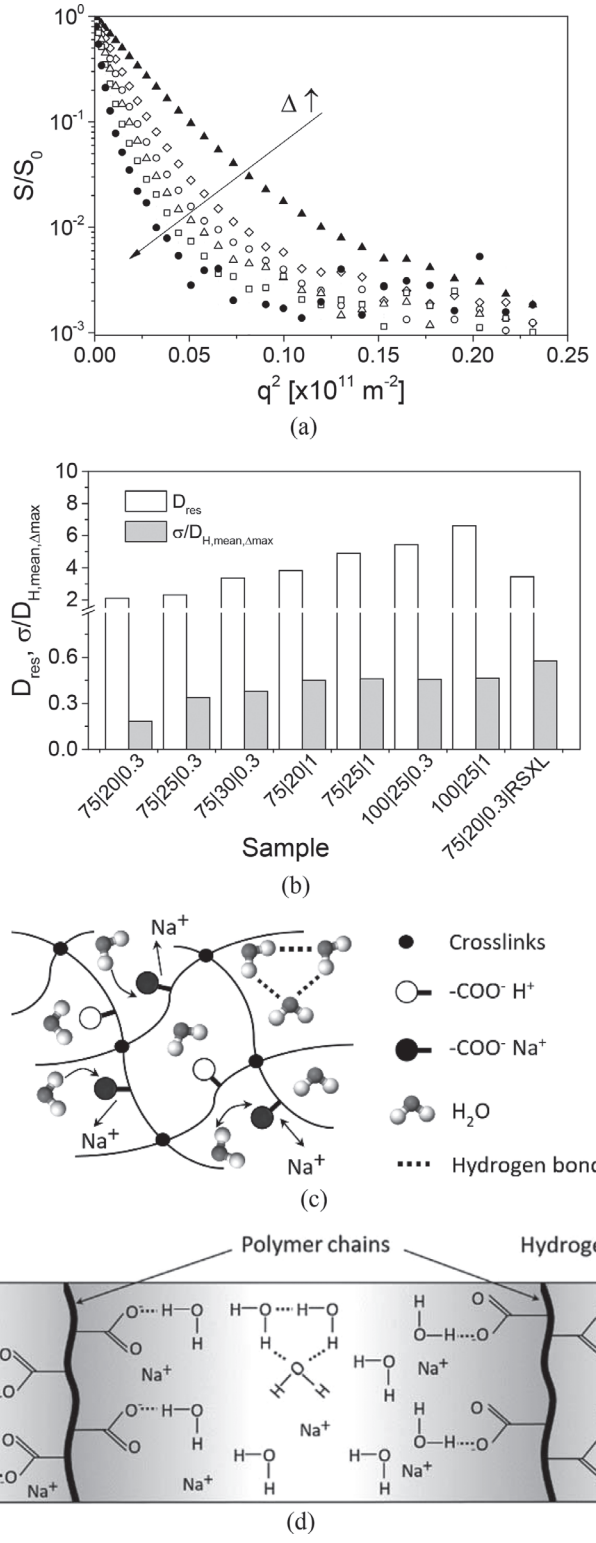

Figure 4. a) Signal decays S/S_0 for ^1H diffusion in a swollen hydrogel (SAP75|20|0.3|RSXL) at different diffusion times (▲: 40; ◊: 80; ○: 120; Δ: 160; □: 240; ●: 480 ms); b) ^1H relative distribution width of diffusion $\sigma/D_{H,mean,\Delta max}$ and D_{res} (residual ^1H-^1H dipolar coupling determined by ^1H DQ-NMR). Adapted with permission.[9] Copyright 2018, Wiley-VCH; c) schematic representation of a SAP hydrogel, hydrogen bonds, hydration of carboxylic group and $^{23}Na^+$, and the release of $^{23}Na^+$ during swelling; d) simplified model of water-mobility in the area between two chains in a swollen hydrogel. The distance between polymer segments changes with the swelling degree. H_2O and $^{23}Na^+$ move around because of the Brownian motion.

negatively charged carboxylic groups. The polymeric backbone can be modeled as a semi rod-like segment (Figure 4d). H^+ and Na^+ ions come into contact with the polymer chains due to electrostatic interactions.[6] In addition, the carboxylic group and $^{23}Na^+$ attract H_2O and form a hydration complex, for example, water-shell structures.[47] In general, the degree of hydration of Na^+ ions in the swollen hydrogel depends on the degree of neutralization and the swelling degree. For the hydrogels with DN = 100%, $–COO^-$ H^+ are "neutralized" into $–COO^-$ Na^+. Besides the hydrogen bonds between hydrogen atoms of water and -COO^- groups, water molecules also form water-shell structures by means of electron pairs between Na^+ ions and oxygen atoms of water (Figure 4c,d). At very low swelling degree or water content, two oxygen atoms in carboxylic group tend to coordinate a Na^+ in octet coordination.[48] In such an octet coordination one Na^+ will be coordinated by four water molecules.[49] If a dissociated Na^+ is only surrounded by water, the maximum coordination number will be 6 in the octet coordination model. Due to the electrostatic interaction and/or hydrogen bonds, water molecules will continue to form the hydration shell gradually. With further increase of swelling degree or water content, free or bulk water molecules are in the swollen gels. In Manning's condensation theory for an infinitely long cylindrical polyion,[50,51] the condensed counterions are assumed to show a vanishing mobility, while the uncondensed counterions and all co-ions are subjected to Brownian motion in the inhomogeneous electric field created by the polyelectrolyte molecules. Experimentally, binding effects can be probed by NMR spectroscopy, transport, and thermodynamic methods.[52,53] The two-state Manning condensation and its extended two-zone model were often used to describe bound and free metal ions in polyelectrolyte solutions.[52,54,55] Similar two-region models were also applied to describe apparent diffusion coefficients and water mobility in contact lenses[56] as well as hydration and ion binding in polyelectrolytes.[47]

Ions (i.e., $^{23}Na^+$, $^1H^+$) in the vicinity of a polymer chain are more or less free to move on longer time scales. The two-state approximation seems to be an oversimplification. The finding that the time-dependent ^1H diffusion is better described by a distribution is a strong indication already. H_2O and $^{23}Na^+$ move around, which is observable on the typical timescales of PFG-NMR experiments. H_2O molecules close to the chain probably move more slowly than those far away from the polymer chain (Figure 4d). The mobility of H_2O in the swollen hydrogels is approximated by a distribution function due to interactions like steric hindrance and hydration. The hydration depends on the gel network and the charge distribution. The mobility of water in the hydrated region is lower, also leading to a wider distribution of water diffusion (Figure 4b). These findings are in accordance with previous DQ experiments on the same samples,[9] where DQ residual dipolar couplings have been probed on a much smaller length scale (^1H-^1H dipolar coupling on Angstrom scale).

For SAPs studied at different swelling degrees, the mean diffusion distance l_z travelled by H_2O during $\Delta \in [40, 480]$ ms is in the range $l_z \in [10, 40]$ μm, while l_z of pure water amounts to 50 µm. l_z increases with Q. Moreover, gels with a higher degree of crosslinking or with surface crosslinking show smaller l_z due to the stronger steric hindrance. The typical mesh size is 1–10 nm, the typical length scale of spatial inhomogeneity of the polymer crosslinking density is in the range of 10–100 nm.[46] PFG-NMR diffusion has been studied on the length scale of a few tens of micrometers, which means that average quantities have been observed.[44]

3.4. Sodium Relaxation and Its Relation to Sodium Diffusion, Structural and Synthesis Parameters of SAP Hydrogels

The $^{23}Na^+$ translational mobility is influenced by the above discussed interactions in the swollen SAP gels (cf. Section 3.3). ^{23}Na-NMR relaxation on the swollen SAPs was measured at different swelling degrees. Longitudinal and transverse relaxation of a spin-3/2 nucleus depend not only on fluctuating spin–spin interactions but also on the fluctuating electric field gradient. The quadrupolar interactions fluctuate fast on the time scale of the NMR experiment (Figure 1a). In ^{23}Na-relaxation experiments, relaxation decays and magnetization build-up curves are describable with mono-exponentials. $^{23}Na^+$ in the swollen hydrogels therefore experience fast fluctuating quadrupolar interactions on the frequency scales of Larmor frequency and of a few kHz leading to quadrupolar relaxation.

The $^{23}Na^+$ relaxation rates R_1 and R_2 increase with decreasing swelling degree (**Figure 5**). The polymer chains become more compact at a lower swelling degree, and thus the vibrational frequencies, that is, correlation times of the quadrupolar interactions, change together with an increased probability of entanglement. The dilute NaCl solution thus exhibits longer relaxation times of $^{23}Na^+$ (T_1 = 49.6 ms and T_2 = 34 ms). It is interesting that the measured $^{23}Na^+$ relaxation rates for samples with DN = 100% are larger than those with DN = 75% (cf. SAP**75**|25|0.3 vs SAP**100**|25|0.3 and SAP**75**|25|1 vs SAP**100**|25|1 in Figure 5). The increase of the relaxation rates with DN is related to a higher $^{23}Na^+$ concentration and stiffer gel. It is noteworthy that the neutralized hydrogel chains contain negative charges which repel each other and are balanced by positive ions (Figure 4c,d). $^{23}Na^+$ are hydrated which reduces the electrostatic attraction to carboxylate ions, allowing the hydrated $^{23}Na^+$ to move relatively fast within the network.[6,57] $^{23}Na^+$ are still attracted by the negative carboxylate groups and exchange with other ions (Figure 4c,d). The strength of such an ion trap and the local ion-exchange dynamics on the timescale of ms are reflected in R_2, while R_1 indicates fluctuations in the frequency range of about 106 MHz in the current experiment. Faster relaxation rates R_1 and R_2 are observed with a stronger effect on the latter.[58,59] The samples with higher DC show slightly faster ^{23}Na relaxation rates (SAP75|20|**0.3** vs SAP75|20|**1**, SAP75|25|**0.3** vs SAP75|25|**1**, and SAP100|25|**0.3** vs SAP100|25|**1** in Figure 5). However, no significant difference between the relaxation rates measured for different swelling degrees was observed for the samples with the same DN and DC (SAP75|**20**|0.3 vs SAP75|**25**|0.3 and SAP75|**20**|1 vs SAP75|**25**|1 in Figure 5), except that SAP75|30|0.3 shows somewhat smaller values of R_1 and R_2. A higher monomer concentration results in a larger fraction of polymer chains and thus possibly more physical crosslinks as chemically fixed entanglements. After swelling,

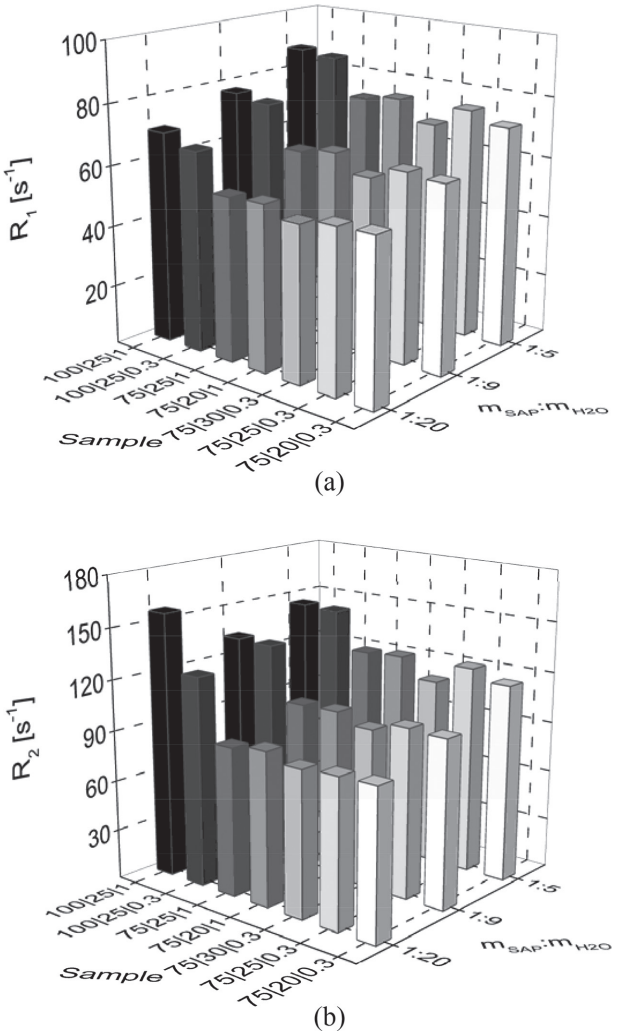

Figure 5. ^{23}Na relaxation rates a) R_1 and b) R_2 for hydrogels at three different swelling degrees ($m_{SAP}:m_{H_2O}$ = 1:5, 1:9, and 1:20).

electrostatic repulsion and hydration may lead to a redistribution of $^{23}Na^+$ in the swollen gel, that is, a release of $^{23}Na^+$ into regions away from the polymer chains (Figure 4d). Thus the hydrogel SAP75|30|0.3 gives rise to somewhat shorter R_1 and R_2 and a somewhat larger diffusion coefficient (Figures 2a, 5, and 6).

Translational ^{23}Na-NMR diffusion and relaxation rates were compared for the SAP hydrogels and related to structural and synthesis parameters at $m_{SAP}:m_{H_2O}$ = 1:9 (**Figure 6**). Among hydrogels without surface crosslinking, both diffusion coefficients and relaxation times ($T_i = 1/R_i$) of $^{23}Na^+$ indicate similar trends with the synthesis parameters. The overall diffusion coefficient of $^{23}Na^+$ in SAP75|20|0.3|RSXL is smaller, whereas D_{res} is larger than that without surface crosslinking (SAP75|20|0.3) due to the contribution from the high surface crosslinking density. Regarding the relaxation rates, however, there is only a small difference between the two hydrogels. An increase in D_{res} tends to an increase in relaxation rates and a reduction in the $^{23}Na^+$ diffusion coefficient. D_{res} corresponds

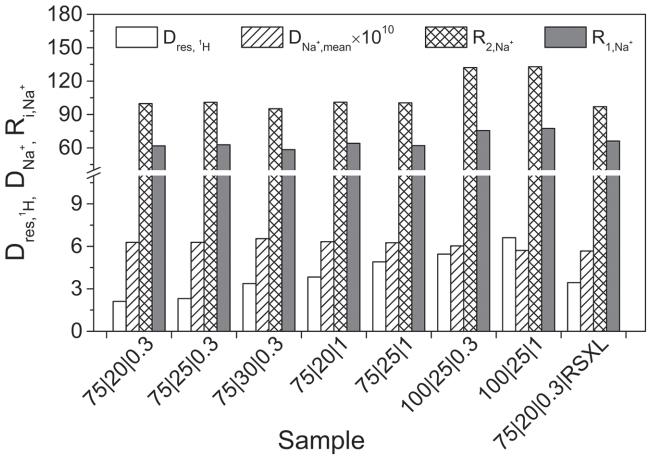

Figure 6. ^{23}Na-NMR diffusion and relaxation rates at $m_{SAP}:m_{H_2O}$ = 1:9 together with ^{1}H D_{res}. Adapted with permission.[9] Copyright 2018, Wiley-VCH.

to structural changes of hydrogels, while DN has the highest impact on relaxation.

To further look into $^{23}Na^+$ dynamics, diffusion coefficients and relaxation rates were correlated while swelling degree is an intrinsic variable (**Figure 7**). With increasing Q, $D_{Na^+,mean}$ increases linearly but is much smaller than in 0.1 M NaCl, while both relaxation rates decrease. As expected, R_2 in swollen hydrogels is faster than R_1 by a factor of about 1.6. In samples with larger DN $D_{Na^+,mean}$ is smaller, while relaxation rates are larger (Figure 7). Experimental data for hydrogels with surface crosslinking almost coincide with the linear relation between $D_{Na^+,mean}$ and R_1 (or R_2) for SAP without surface crosslinking, because the core-shell hydrogels have the same core crosslink density as those without surface crosslinking. In previous DQ-NMR experiments,[9] the fractions of network chains and

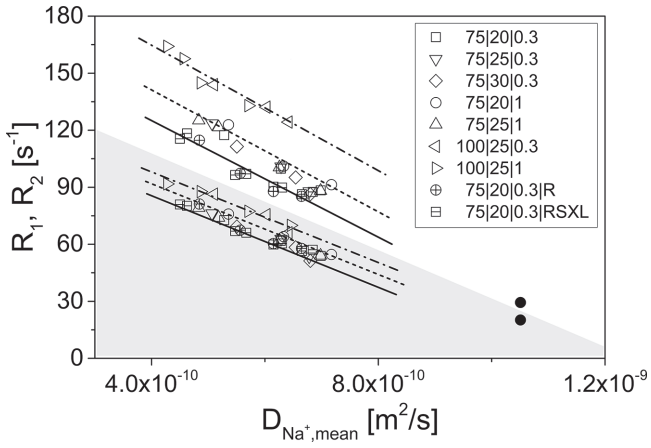

Figure 7. Correlation between ^{23}Na diffusion and ^{23}Na relaxation for SAPs at different swelling degrees (indicated by the symbols in Table 1). Corresponding values of 0.1 M NaCl solution (●) are also given for comparison. Symbols represent the experimental data, and lines are guides to the eye (---: DN = 100%; ----: DN = 75% and DC = 1%; —: DN = 75% and DC = 0.3%). The data in the lower grey-marked area correspond to R_1, data in the upper white area R_2.

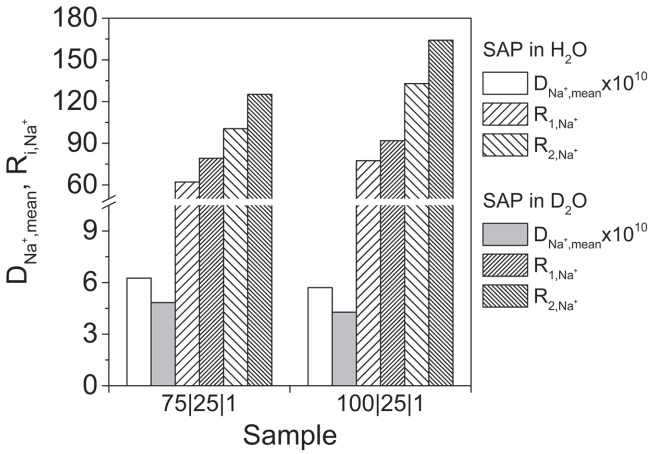

Figure 8. Comparison of $^{23}Na^+$ diffusion coefficients and relaxation rates in two hydrogel samples (SAP75|25|1 and SAP100|25|1) swollen in D_2O and H_2O.

defects were found to be constant for SAP gels with and without surface crosslinking, but hydrogels with surface crosslinking tend to have a broader or even bimodal RDC distribution and thus a large mean D_{res} (Figure 6). $^{23}Na^+$ in the swollen gels with and without surface crosslinking are in a similar state at the same swelling degree except for the overall diffusion coefficient which reflects the hindrance by surface crosslinking. For hydrogels with the same DN and DC at the same swelling degree, the difference is very small. A trend is observed for relaxation rates which increase with DC (solid and dashed lines in Figure 7).

Pearson correlation analysis indicates that the correlations are significant at the 0.05 level. The correlation coefficients between $D_{Na^+,mean}$ and R_1 are − 0.8710, − 0.9876, and − 0.9785 for SAPs with DN = 100%, SAPs with DN = 75% and DC = 1% and SAPs with DN = 75% and DC = 0.3%, respectively. Similarly, the correlation coefficients between $D_{Na^+,mean}$ and R_2 are − 0.9738, − 0.9816 , and − 0.8817 for SAPs with DN = 100%, SAPs with DN = 75% and DC = 1% and SAPs with DN = 75% and DC = 0.3%, respectively. The correlation coefficients are in the range between − 0.8710 and − 0.9876, implying that $D_{Na^+,mean}$ and R_1 (or R_2) are well linearly related in the measured range.

Additional experiments were performed by swelling the SAP in D_2O. $^{23}Na^+$ diffusion coefficients (D_2O) are smaller than those observed in H_2O swollen hydrogels, but relaxation rates are larger (**Figure 8**). This is attributed to the larger viscosity of D_2O ($\eta_{D_2O} \approx 1.232 \times \eta_{H_2O}$ at 25 °C).[60] ^{23}Na relaxation rates were found to be proportional to the viscosity of the swelling solvent.[61] Although liquid D_2O and H_2O have very similar molecular properties and the molecules tend to be oriented with the oxygen toward $^{23}Na^+$, D_2O shows more stable hydrogen bonds than H_2O because of its higher zero-point energy of intermolecular vibrations.[62,63] Those properties are reflected in $^{23}Na^+$diffusion and relaxation: The ratios of diffusion coefficients $(D_{Na^+,mean})_{H_2O}/(D_{Na^+,mean})_{D_2O}$ and relaxation rates $(R_{i,Na^+})_{D_2O}/(R_{i,Na^+})_{H_2O}$ for hydrogels swollen in H_2O and D_2O amount to 1.2–1.3, which is close to the viscosity ratio of D_2O to H_2O (1.23).

4. Conclusions

Superabsorbent polymer hydrogels have been investigated by ^1H and ^{23}Na PFG-NMR diffusion and ^{23}Na-NMR relaxation. $^{23}Na^+$ and ^1H diffusion coefficients are both reduced. A gamma distribution model was used to analyze PFG-NMR data. $D_{H,mean}$ decrease with diffusion time, which is an indication for geometrical hindrance and molecular interactions. The distribution width appears to be a valuable measure, too. ^{23}Na-NMR relaxation and diffusion reveal insight into motional dynamics of $^{23}Na^+$ in the swollen hydrogels. $D_{Na^+,mean}$ is nearly constant in the interval of diffusion times $\Delta \in [7,30]$ ms and smaller than $D_{H,mean}$ at the same swelling degree. $^{23}Na^+$ in swollen hydrogels are in the fast motional regime of NMR. A higher degree of neutralization causes faster ^{23}Na relaxation and smaller diffusion. Surface crosslinking also hinders ^{23}Na diffusion. Only a small difference in ^{23}Na relaxation is observed for hydrogels with and without surface crosslinking. ^{23}Na diffusion for SAP hydrogels swollen in D_2O is smaller than in H_2O but relaxation rates are larger. The ratios of the corresponding NMR values in both cases (diffusion coefficients and relaxation times) are close to the viscosity ratio of D_2O to H_2O (1.23). For hydrogels with the same degrees of neutralization and crosslinking at the same swelling degree, the difference between ^{23}Na relaxation rates is very small. However, relaxation rates lightly increase with the degree of crosslinking. $^{23}Na^+$ relaxation rates R_1 and R_2 tend to decrease as $D_{Na^+,mean}$ increases. An extension to other cations is of interest for material development, which will be investigated in future work.

Acknowledgements

Financial support from the German Research Foundation (DFG SFB 1176 Project Q2 as well as Pro²NMR instrumental facility at KIT and RWTH Aachen) is highly appreciated. The authors would like to thank the reviewers for their comments and suggestions regarding the description of diffusion data.

Conflict of Interest

The authors declare no conflict of interest.

Keywords

^{23}Na-NMR, hindered diffusion, hydrogels, pulsed field gradient NMR, superabsorbent polymers

[1] F. L. Buchholz, A. T. Graham, *Modern Superabsorbent Polymer Technology*, Wiley-VCH, New York **1998**.
[2] M. J. Zohuriaan-Mehr, H. Omidian, S. Doroudiani, K. Kabiri, *J. Mater. Sci.* **2010**, *45*, 5711.
[3] K. Kosemund, H. Schlatter, J. L. Ochsenhirt, E. L. Krause, D. S. Marsman, G. N. Erasala, *Regul. Toxicol. Pharmacol.* **2009**, *53*, 81.

[4] S. Jockusch, N. J. Turro, Y. Mitsukami, M. Matsumoto, T. Iwamura, T. Lindner, A. Flohr, G. di Massimo, *J. Appl. Polym. Sci.* **2009**, *111*, 2163.
[5] R. Paul, *Functional Finishes for Textiles: Improving Comfort, Performance and Protection*, Elsevier Science, Amsterdam **2014**.
[6] M. Elliott, *Superabsorbent Polymers, BASF-Ag.* **2004**.
[7] L. Masaro, X. X. Zhu, *Prog. Polym. Sci.* **1999**, *24*, 731.
[8] A. H. Muhr, J. M. V. Blanshard, *Polymer* **1982**, *23*, 1012.
[9] X. Guo, S. Theissen, J. Claussen, V. Hildebrand, J. Kamphus, M. Wilhelm, B. Luy, G. Guthausen, *Macromol. Chem. Phys.* **2018**, *219*, 1800100.
[10] J. Höpfner, G. Guthausen, K. Saalwächter, M. Wilhelm*Macromolecules* **2014**, *47*, 4251.
[11] W. S. Price, *NMR Studies of Translational Motion: Principles and Applications*, Cambridge University Press, Cambridge **2009**.
[12] C. S. Johnson, *Prog. Nucl. Magn. Reson. Spectrosc.* **1999**, *34*, 203.
[13] S. Matsukawa, H. Yasunaga, C. Zhao, S. Kuroki, H. Kurosu, I. Ando, *Prog. Polym. Sci.* **1999**, *24*, 995.
[14] R. Roque-Malherbe, *Adsorption and Diffusion in Nanoporous Materials*, CRC Press, Boca Raton **2007**.
[15] J. Kärger, D. M. Ruthven, *New J. Chem.* **2016**, *40*, 4027.
[16] J. Kärger, D. M. Ruthven, D. N. Theodorou, *Diffusion in Nanoporous Materials*, Wiley-VCH, Weinheim **2012**.
[17] J. Kärger, D. M. Ruthven, *Diffusion in Zeolites and Other Microporous Solids*, Wiley, New York **1992**.
[18] L. Zeng, E. O. Stejskal, *Appl. Spectrosc.* **1996**, *50*, 1402.
[19] E. O. Stejskal, J. E. Tanner, *J. Chem. Phys.* **1965**, *42*, 288.
[20] X. Guo, E. Laryea, M. Wilhelm, B. Luy, H. Nirschl, G. Guthausen, *Macromol. Chem. Phys.* **2017**, *218*, 1600440.
[21] M. Röding, D. Bernin, J. Jonasson, A. Sarkka, D. Topgaard, M. Rudemo, M. Nyden, *J. Magn. Reson.* **2012**, *222*, 105.
[22] H. Y. Carr, E. M. Purcell, *Phys. Rev.* **1954**, *94*, 630.
[23] S. Meiboom, D. Gill, *Rev. Sci. Instrum.* **1958**, *29*, 688.
[24] P. Passiniemi, S. Liukkonen, Z. Noszticzius, *J. Chem. Soc., Faraday Trans. 1* **1977**, *73*, 1834.
[25] P. Passiniemi, *J. Solution Chem.* **1983**, *12*, 801.
[26] M. Ohuchi, P. Meadows, H. Horiuchi, Y. Sakai, K. Furihata, *Polym. J.* **2000**, *32*, 760.
[27] M. Muthukumar, *J. Chem. Phys.* **2004**, *120*, 9343.
[28] S. Liu, K. Ghosh, M. Muthukumar, *J. Chem. Phys.* **2003**, *119*, 1813.
[29] R. Coşkun, M. Yi˙ği˙toğlu, M. Saçak, *J. Appl. Polym. Sci.* **2000**, *75*, 766.
[30] E. O. Ningrum, A. Purwanto, E. O. Mulyadi, D. I. Dewitasari, S. Sumarno, *Indones. J. Chem.* **2017**, *17*, 446.
[31] M. Holz, S. R. Heil, A. Sacco, *Phys. Chem. Chem. Phys.* **2000**, *2*, 4740.
[32] H. Yasunaga, I. Ando, *Polym. Gels Networks* **1993**, *1*, 83.
[33] H. Yasunaga, I. Ando, *Polym. Gels Networks* **1993**, *1*, 267.
[34] L. L. Latour, P. P. Mitra, R. L. Kleinberg, C. H. Sotak, *J. Magn. Reson., Ser. A* **1993**, *101*, 342.
[35] L. Pisani, *Transp. Porous Media* **2011**, *88*, 193.
[36] B. Ghanbarian, A. G. Hunt, R. P. Ewing, M. Sahimi, *Soil Sci. Soc. Am. J.* **2013**, *77*, 1461.
[37] L. L. Latour, R. L. Kleinberg, P. P. Mitra, C. H. Sotak, *J. Magn. Reson., Ser. A* **1995**, *112*, 83.
[38] L. J. Barbour, *Chem. Commun.* **2006**, *11*, 1163.
[39] M. Sánchez-Serratos, J. R. Álvarez, E. González-Zamora, I. A. Ibarra, *J. Mex. Chem. Soc.* **2016**, *60*, 43.
[40] D. W. de Kort, J. P. M. van Duynhoven, H. Van As, F. Mariette, *Trends Food Sci. Technol.* **2015**, *42*, 13.
[41] H. Fujita, *Fortschr. Hochpolym. Forsch.* **1961**, *3*, 1.
[42] J. S. Vrentas, J. L. Duda, *J. Polym. Sci., Polym. Phys. Ed.* **1977**, *15*, 403.
[43] J. M. Petit, B. Roux, X. X. Zhu, P. M. Macdonald, *Macromolecules* **1996**, *29*, 6031.
[44] G. Modesti, B. Zimmermann, M. Börsch, A. Herrmann, K. Saalwächter, *Macromolecules* **2009**, *42*, 4681.
[45] P. Lundberg, P. W. Kuchel, *Magn. Reson. Med.* **1997**, *37*, 44.
[46] F. Di Lorenzo, S. Seiffert, *Polym. Chem.* **2015**, *6*, 5515.
[47] A. Ikegami, *J. Polym. Sci. A* **1964**, *2*, 907.
[48] K. Hiraoka, T. Yokoyama, *Polym. Bull.* **1980**, *2*, 183.
[49] K. Hiraoka, H. Shin, T. Yokoyama, *Polym. Bull.* **1982**, *8*, 303.
[50] G. S. Manning, *J. Chem. Phys.* **1969**, *51*, 924.
[51] G. S. Manning, *J. Chem. Phys.* **1969**, *51*, 934.
[52] P. Stilbs, B. Lindman, *J. Magn. Reson.* **1982**, *48*, 132.
[53] G. Gunnarsson, B. Joensson, H. Wennerstroem, *J. Phys. Chem.* **1980**, *84*, 3114.
[54] M. S. Palencia, B. L. Rivas, E. D. Pereira, *Polym. Int.* **2010**, *59*, 1542.
[55] A. V. Dobrynin, M. Rubinstein, *Prog. Polym. Sci.* **2005**, *30*, 1049.
[56] C. Manetti, L. Casciani, N. Pescosolido, *J. Biomater. Sci., Polym. Ed.* **2004**, *15*, 331.
[57] G. Korotcenkov, *Handbook of Humidity Measurement, Volume 1: Spectroscopic Methods of Humidity Measurement*, CRC Press, Boca Raton **2018**.
[58] M. Raue, A. Bernet, M. Küppers, S. Stapf, H.-W. Schmidt, B. Blümich, T. Mang, in *Intelligent Hydrogels, Progress in Colloid and Polymer Science 140* (Eds: G. Sadowski, W. Richtering), Springer International Publishing, Cham, Switzerland **2013**, p. 45.
[59] D. E. Woessner, *Concepts Magn. Reson.* **2001**, *13*, 294.
[60] W. N. Baker, *J. Chem. Phys.* **1936**, *4*, 294.
[61] M. Eisenstadt, H. L. Friedman, *J. Chem. Phys.* **1966**, *44*, 1407.
[62] D. Eisenberg, D. S. Eisenberg, W. Kauzmann, *The Structure and Properties of Water*, Oxford University Press, Oxford **2005**.
[63] G. Némethy, H. A. Scheraga, *J. Chem. Phys.* **1964**, *41*, 680.